

**Space-Time Finite Element Methods
for Parabolic Evolution Problems with
Non-smooth Solutions**

Ulrich Langer Andreas Schafelner

DK-Report No. 2019-03

03 2019

A-4040 LINZ, ALTENBERGERSTRASSE 69, AUSTRIA

Supported by

Austrian Science Fund (FWF)

Upper Austria

Editorial Board: Bruno Buchberger
Evelyn Buckwar
Bert Jüttler
Ulrich Langer
Manuel Kauers
Peter Paule
Veronika Pillwein
Silviu Radu
Ronny Ramlau
Josef Schicho

Managing Editor: Diego Dominici

Communicated by: Bert Jüttler
Veronika Pillwein

DK sponsors:

- **Johannes Kepler University Linz (JKU)**
- **Austrian Science Fund (FWF)**
- **Upper Austria**

Space-Time Finite Element Methods for Parabolic Evolution Problems with Non-smooth Solutions*

Ulrich Langer[†] Andreas Schafelner[‡]

March 5, 2019

Abstract

We propose consistent locally stabilized, conforming finite element schemes on completely unstructured simplicial space-time meshes for the numerical solution of non-autonomous parabolic evolution problems under the assumption of maximal parabolic regularity. We present new a priori estimates for low-regularity solutions. In order to avoid reduced convergence rates appearing in the case of uniform mesh refinement, we also consider adaptive refinement procedures based on residual a posteriori error indicators. The huge system of space-time finite element equations is then solved by means of GMRES preconditioned by algebraic multigrid.

1 Introduction

Parabolic initial-boundary value problems of the form

$$\partial_t u - \operatorname{div}_x(\nu \nabla_x u) = f \text{ in } Q, \quad u = 0 \text{ on } \Sigma, \quad u = u_0 \text{ on } \Sigma_0 \quad (1)$$

describe not only heat conduction and diffusion processes but also 2D eddy current problems in electromagnetics and many other evolution processes, where $Q = \Omega \times (0, T)$, $\Sigma = \partial\Omega \times (0, T)$, and $\Sigma_0 = \Omega \times \{0\}$ denote the space-time cylinder, its lateral boundary, and the bottom face, respectively. The spatial computational domain $\Omega \subset \mathbb{R}^d$, $d = 1, 2, 3$, is supposed to be bounded and Lipschitz. The final time is denoted by T . The right-hand side f is a given source function from $L_2(Q)$. The given coefficient ν may depend on the spatial variable x as well as the time variable t . In the latter case, the problem is called non-autonomous. We suppose at least that ν is uniformly positive and bounded almost everywhere. We here consider homogeneous Dirichlet boundary

*Supported by the Austrian Science Fund (FWF) under the grant W1214, project DK4.

[†]Institute for Computational Mathematics, Johannes Kepler University Linz.

[‡]Doctoral Program Computational Mathematics, Johannes Kepler University Linz.

conditions for the sake of simplicity. In practice, we often meet mixed boundary conditions. Discontinuous coefficients, non-smooth boundaries, changing boundary conditions, non-smooth or incompatible initial conditions, and non-smooth right-hand sides can lead to non-smooth solutions.

In contrast to the conventional time-stepping methods in combination with some spatial discretization method, or the more advanced, but closely related discontinuous Galerkin (dG) methods based on time slices, we here consider space-time finite element discretizations treating time as just another variable and the term $\partial_t u$ in (1) as convection term in time. Following [8], we derive consistent, locally stabilized, conforming finite element schemes on completely unstructured simplicial space-time meshes under the assumption of maximal parabolic regularity; see, e.g., [6]. Unstructured space-time schemes have clear advantages with respect to adaptivity, parallelization, and the numerical treatment of moving interfaces or special domains. We refer the reader to the survey paper [10] that provides an excellent overview of completely unstructured space-time methods and simultaneous space-time adaptivity. In particular, we would like to mention the papers [9] that is based on an inf-sup-condition, [4] that uses mesh-grading in time, and [1] that also uses stabilization techniques. All three papers treat the autonomous case.

We here present new a priori discretization error estimates for low-regularity solutions. In order to avoid reduced convergence rates appearing in the case of uniform mesh refinement, we also consider adaptive refinement procedures in the numerical experiments presented in Section 5. The adaptive refinement procedures are based on residual a posteriori error indicators. The huge system of space-time finite element equations is then solved by means of Generalized Minimal Residual Method (GMRES) preconditioned by an algebraic multigrid cycle. In particular, in the 4D space-time case that is 3D in space, simultaneous space-time adaptivity and parallelization can considerably reduce the computational time. The space-time finite element solver was implemented in the framework of MFEM. The numerical results nicely confirm our theoretical findings. The parallel version of the code shows an excellent parallel performance.

2 Weak formulation and maximal parabolic regularity

The weak formulation of the model problem (1) reads as follows: find $u \in H_0^{1,0}(Q) := \{u \in L_2(Q) : \nabla_x u \in [L_2(Q)]^d, u = 0 \text{ on } \Sigma\}$ such that (s.t.)

$$\int_Q (-u \partial_t v + \nu \nabla_x u \cdot \nabla_x v) \, d(x, t) = \int_Q f v \, d(x, t) + \int_\Omega u_0 v|_{t=0} \, dx \quad (2)$$

for all $v \in \hat{H}_0^1(Q) = \{u \in H^1(Q) : u = 0 \text{ on } \Sigma \cup \Sigma_T\}$, where $\Sigma_T := \Omega \times \{T\}$. The existence and uniqueness of weak solutions is well understood; see, e.g., [7]. It was already shown in [7] that $\partial_t u \in L^2(Q)$ and $\Delta u \in L^2(Q)$ provided that $\nu = 1$, $f \in L^2(Q)$, and $u_0 = 0$. This case is called maximal parabolic regularity.

Similar results can be obtained under more general assumptions imposed on the data; see, e.g., [6] for some very recent results on the non-autonomous case.

3 Locally stabilized space-time finite element methods

In order to derive the space-time finite element scheme, we need an admissible, shape regular decomposition $\mathcal{T}_h = \{K\}$ of the space-time cylinder $Q = \bigcup_{K \in \mathcal{T}_h} \overline{K}$ into finite elements K . On \mathcal{T}_h , we define a H^1 conforming finite element space V_h by means of polynomial simplicial finite elements of the degree p in the usual way; see, e.g., [2]. Let us assume that the solution u of (2) belongs to the space $V_0 = H_{0,0}^{\mathcal{L},1}(\mathcal{T}_h) := \{u \in L_2(Q) : \partial_t u \in L_2(K), \mathcal{L}u := \operatorname{div}_x(\nu \nabla_x u) \in L_2(K) \forall K \in \mathcal{T}_h, \text{ and } u|_{\Sigma \cup \Sigma_0} = 0\}$, i.e., we only need some local version of maximal parabolic regularity, and, for simplicity, we assume homogeneous initial conditions, i.e., $u_0 = 0$. Multiplying the PDE (1) on K by a local time-upwind test function $v_h + \theta_K h_K \partial_t v_h$, with $v_h \in V_{0h} = \{v_h \in V_h : v_h = 0 \text{ on } \Sigma \cup \Sigma_0\}$, $h_K = \operatorname{diam}(K)$, and a parameter $\theta_K > 0$ which we will specify later, integrating over K , integrating by parts, and summing up over all elements $K \in \mathcal{T}_h$, we arrive at the following consistent space-time finite element scheme: find $u_h \in V_{0h}$ s.t.

$$a_h(u_h, v_h) = l_h(v_h), \quad \forall v_h \in V_{0h}, \quad (3)$$

with

$$\begin{aligned} a_h(u_h, v_h) &= \sum_{K \in \mathcal{T}_h} \int_K [\partial_t u_h v_h + \theta_K h_K \partial_t u_h \partial_t v_h \\ &\quad + \nu \nabla_x u_h \cdot \nabla_x v_h - \theta_K h_K \operatorname{div}_x(\nu \nabla_x u_h) \partial_t v_h] d(x, t), \\ l_h(v_h) &= \sum_{K \in \mathcal{T}_h} \int_K f v_h + \theta_K h_K f \partial_t v_h d(x, t). \end{aligned} \quad (4)$$

$$(5)$$

The bilinearform $a_h(\cdot, \cdot)$ is coercive on $V_{0h} \times V_{0h}$ wrt to the norm

$$\|v\|_h^2 = \frac{1}{2} \|v\|_{L_2(\Sigma_T)}^2 + \sum_{K \in \mathcal{T}_h} \left[\theta_K h_K \|\partial_t v\|_{L_2(K)}^2 + \|\nabla_x v\|_{L_2^y(K)}^2 \right], \quad (6)$$

i.e., $a_h(v_h, v_h) \geq \mu_c \|v_h\|_h^2$, $\forall v_h \in V_{0h}$, and bounded on $V_{0h,*} \times V_{0h}$ wrt to the norm

$$\|v\|_{h,*}^2 = \|v\|_h^2 + \sum_{K \in \mathcal{T}_h} \left[(\theta_K h_K)^{-1} \|v\|_{L_2(K)}^2 + \theta_K h_K \|\operatorname{div}_x(\nu \nabla_x v)\|_{L_2(K)}^2 \right], \quad (7)$$

i.e., $a_h(u_h, v_h) \leq \mu_b \|u_h\|_{h,*} \|v_h\|_h$, $\forall u_h \in V_{0h,*}, \forall v_h \in V_{0h}$, where $V_{0h,*} := H_{0,0}^{\mathcal{L},1}(Q) + V_{0h}$; see [8, Lemma 3.8] and [8, Remark 3.13], respectively. The coercivity constant μ_c is robust in h_K provided that we choose $\theta_K = \mathcal{O}(h_K)$;

see Section 5 or [8, Lemma 3.8] for the explicit choice. From the above derivation of the scheme, we get consistency $a_h(u, v_h) = l_h(v_h)$, $\forall v_h \in V_{0h}$, provided that the solution u belongs to $H_{0,0}^{\mathcal{L},1}(Q)$ that is ensured in the case of maximal parabolic regularity. The space-time finite element scheme (3) and the consistency relation immediately yield Galerkin orthogonality

$$a_h(u - u_h, v_h) = 0, \quad \forall v_h \in V_{0h}. \quad (8)$$

We deduce that (3) is nothing but a huge linear system of algebraic equations. Indeed, let $V_{0h} = \text{span}\{p^{(j)}, j = 1, \dots, N_h\}$, where $\{p^{(j)}, j = 1, \dots, N_h\}$ is the nodal finite element basis and N_h is the total number of space-time degrees of freedom (dofs). Then we can express each function in V_{0h} in terms of this basis, i.e., we can identify each finite element function $v_h \in V_{0h}$ with its coefficient vector $\mathbf{v}_h \in \mathbb{R}^{N_h}$. Moreover, each basis function $p^{(j)}$ is also a valid test function. Hence, we obtain N_h equations from (3), which we rewrite as a system of linear algebraic equations, i.e.

$$\mathbf{K}_h \mathbf{u}_h = \mathbf{f}_h,$$

with the solution vector $\mathbf{u}_h = (u_j)_{j=1, \dots, N_h}$, the vector $\mathbf{f}_h = (l_h(p^{(i)}))_{i=1, \dots, N_h}$, and system matrix $\mathbf{K}_h = (a_h(p^{(j)}, p^{(i)}))_{i,j=1, \dots, N_h}$ that is non-symmetric, but positive definite.

4 A priori discretization error estimates

Galerkin orthogonality (8), together with coercivity and boundedness, enables us to prove a C ea-like estimate, where we bound the discretization error in the $\|\cdot\|_h$ -norm by the best-approximation error in the $\|\cdot\|_{h,*}$ -norm.

Lemma 1. *Let the bilinearform (4) be coercive [8, Lemma 3.8] with constant μ_c and bounded [8, Lemma 3.11, Remark 3.13] with constant μ_b , and let $u \in H_{0,0}^{\mathcal{L},1}(\mathcal{T}_h)$ be the solution of the space-time variational problem (2). Then there holds*

$$\|u - u_h\|_h \leq \left(1 + \frac{\mu_b}{\mu_c}\right) \inf_{v_h \in V_{0h}} \|u - v_h\|_{h,*}, \quad (9)$$

where $u_h \in V_{0h}$ is the solution to the space-time finite element scheme (3).

Proof. Estimate (9) easily follows from triangle inequality and Galerkin-orthogonality; see [8, Lemma 3.15, Remark 3.16] for details. \square

Next, we estimate the best approximation error by the interpolation error, where we have to choose a proper interpolation operator \mathcal{I}_* . For smooth solutions, i.e., $u \in H^l(Q)$ with $l > (d+1)/2$, we obtained a localized a priori error estimate, see [8, Theorem 3.17], where we used the standard Lagrange interpolation operator \mathcal{I}_h ; see e.g. [2]. In this paper, we are interested in non-smooth solutions, which means that we only require $u \in H^l(Q)$, with some real $l > 1$. Hence, we cannot use the Lagrange interpolator. We can, however, use

so-called quasi-interpolators, e.g. Clément [3] or Scott-Zhang [2]. For this kind of operators, we need a neighborhood S_K of an element $K \in \mathcal{T}_h$ which is defined as $S_K := \{K' \in \mathcal{T}_h : \bar{K} \cap \bar{K}' \neq \emptyset\}$. Let $u \in H^l(Q)$, with some real $l > 1$, then, for the Scott-Zhang quasi-interpolation operator $\mathfrak{I}_{SZ} : L_2(Q) \rightarrow V_{0h}$, we have the local estimate (see e.g. [2, (4.8.10)])

$$\|v - \mathfrak{I}_{SZ}v\|_{H^k(K)} \leq C_{\mathfrak{I}_{SZ}} h_K^{l-k} |v|_{H^l(S_K)}, \quad k = 0, 1. \quad (10)$$

For details on the construction of such a quasi-interpolator, we refer to [2] and the references therein. For simplicity, we now assume that the diffusion coefficient ν is piecewise constant, i.e., $\nu|_K = \nu_K$, for all $K \in \mathcal{T}_h$. Then we can show the following lemma.

Lemma 2. *Let $l > 1$ and $v \in V_0 \cap H^l(\mathcal{T}_h)$. Then the following interpolation error estimates are valid:*

$$\|v - \mathfrak{I}_{SZ}v\|_{L_2(\Sigma_T)} \leq c_1 \left(\sum_{\substack{K \in \mathcal{T}_h \\ \partial K \cap \Sigma_T \neq \emptyset}} h_K^{2s-1} |v|_{H^s(K)}^2 \right)^{1/2}, \quad (11)$$

$$\|v - \mathfrak{I}_{SZ}v\|_h \leq c_2 \left(\sum_{K \in \mathcal{T}_h} h_K^{2(s-1)} |v|_{H^s(S_K)}^2 \right)^{1/2}, \quad (12)$$

$$\|v - \mathfrak{I}_{SZ}v\|_{h,*} \leq c_3 \left(\sum_{K \in \mathcal{T}_h} h_K^{2(s-1)} (|v|_{H^s(S_K)}^2 + \|\operatorname{div}_x(\nu \nabla_x v)\|_{L_2(K)}^2) \right)^{1/2}, \quad (13)$$

with $s = \min\{l, p + 1\}$ and positive constants c_1, c_2 and c_3 , that do not depend on v or h_K provided that $\theta_K = \mathcal{O}(h_K)$ for all $K \in \mathcal{T}_h$. Here, p denotes the polynomial degree of the finite element shape functions on the reference element.

Proof. For the first estimate, we use the scaled trace inequality and the quasi-interpolation estimate (10) with $k = 0, 1$

$$\begin{aligned} \|v - \mathfrak{I}_{SZ}v\|_{L_2(\Sigma_T)}^2 &= \sum_{\substack{K \in \mathcal{T}_h \\ \partial K \cap \Sigma_T \neq \emptyset}} \|v - \mathfrak{I}_{SZ}v\|_{L_2(\partial K \cap \Sigma_T)}^2 \leq \sum_{\substack{K \in \mathcal{T}_h \\ \partial K \cap \Sigma_T \neq \emptyset}} \|v - \mathfrak{I}_{SZ}v\|_{L_2(\partial K)}^2 \\ &\leq \sum_{\substack{K \in \mathcal{T}_h \\ \partial K \cap \Sigma_T \neq \emptyset}} [c_{Tr}^2 h_K^{-1} (\|v - \mathfrak{I}_{SZ}v\|_{L_2(K)}^2 + h_K^2 \|\nabla(v - \mathfrak{I}_{SZ}v)\|_{L_2(K)}^2)] \\ &\leq c_{Tr}^2 \sum_{\substack{K \in \mathcal{T}_h \\ \partial K \cap \Sigma_T \neq \emptyset}} [C_{\mathfrak{I}_{SZ}}^2 h_K^{-1} h_K^{2l} |v|_{H^l(S_K)}^2 + C_{\mathfrak{I}_{SZ}}^2 h_K h_K^{2(l-1)} |v|_{H^l(S_K)}^2] \\ &\leq \max_{K \in \mathcal{T}_h} (2 c_{Tr}^2 C_{\mathfrak{I}_{SZ}}^2) \sum_{\substack{K \in \mathcal{T}_h \\ \partial K \cap \Sigma_T \neq \emptyset}} [h_K^{2l-1} |v|_{H^l(S_K)}^2], \end{aligned}$$

which corresponds to (11) with $c_1 = \max_{K \in \mathcal{T}_h} (2 c_{Tr}^2 C_{\mathfrak{I}_{SZ}}^2)$. To show the second estimate (12), we use definition (6) and that ν is piecewise constant, the quasi-interpolation error estimate (10) with $k = 1$, and the above estimate (11), and

obtain

$$\begin{aligned}
& \|v - \mathfrak{I}_{SZ}v\|_h^2 \\
&= \sum_{K \in \mathcal{T}_h} \left[\theta_K h_K \|\partial_t(v - \mathfrak{I}_{SZ}v)\|_{L_2(K)}^2 + \|\nu^{1/2} \nabla_x(v - \mathfrak{I}_{SZ}v)\|_{L_2(K)}^2 \right] \\
&\quad + \frac{1}{2} \|v - \mathfrak{I}_{SZ}v\|_{L_2(\Sigma_T)}^2 \\
&\leq \sum_{K \in \mathcal{T}_h} \left[\theta_K h_K C_{\mathfrak{I}_{SZ}}^2 h_K^{2(l-1)} |v|_{H^l(S_K)}^2 + \nu_K C_{\mathfrak{I}_{SZ}}^2 h_K^{2(l-1)} |v|_{H^l(S_K)}^2 \right] \\
&\quad + c_1 \sum_{\substack{K \in \mathcal{T}_h \\ \partial K \cap \Sigma_T \neq \emptyset}} h_K^{2l-1} |v|_{H^l(S_K)}^2 \\
&\leq \sum_{K \in \mathcal{T}_h} (C_{\mathfrak{I}_{SZ}}^2 (\theta_K h_K + \nu_K) + c_1 h_K) h_K^{2(l-1)} |v|_{H^l(S_K)}^2 \leq c_2 \sum_{K \in \mathcal{T}_h} h_K^{2(l-1)} |v|_{H^l(S_K)}^2,
\end{aligned}$$

with $c_2 = \max_{K \in \mathcal{T}_h} (C_{\mathfrak{I}_{SZ}}^2 (\theta_K h_K + \nu_K) + c_1 h_K)$. For the third estimate, we deduce from (7) that we only have to estimate the additional sum

$$\sum_{K \in \mathcal{T}_h} \left[(\theta_K h_K)^{-1} \|v - \mathfrak{I}_{SZ}v\|_{L_2(K)}^2 + \theta_K h_K \|\operatorname{div}_x(\nu \nabla_x(v - \mathfrak{I}_{SZ}v))\|_{L_2(K)}^2 \right].$$

We start with the first L_2 -term. We apply the quasi-interpolation estimate (10) with $k = 0$ and obtain

$$\begin{aligned}
\sum_{K \in \mathcal{T}_h} (\theta_K h_K)^{-1} \|v - \mathfrak{I}_{SZ}v\|_{L_2(K)}^2 &\leq \sum_{K \in \mathcal{T}_h} (\theta_K h_K)^{-1} C_{\mathfrak{I}_{SZ}}^2 h_K^{2l} |v|_{H^l(S_K)}^2 \\
&\leq \sum_{K \in \mathcal{T}_h} C_{\mathfrak{I}_{SZ}}^2 \left(\frac{h_K}{\theta_K} \right) h_K^{2(l-1)} |v|_{H^l(S_K)}^2.
\end{aligned}$$

Note that the term (h_K/θ_K) is bounded for $\theta_K = \mathcal{O}(h_K)$. For the L_2 -norm of the spatial divergence, we can distinguish between two cases: linear basis functions ($p = 1$) and higher order basis functions ($p \geq 2$). For linear basis functions, we split the divergence of the gradient, obtaining

$$\|\operatorname{div}_x(\nu \nabla_x(v - \mathfrak{I}_{SZ}v))\|_{L_2(K)}^2 = \|\operatorname{div}_x(\nu \nabla_x v) - \operatorname{div}_x(\nu \nabla_x(\mathfrak{I}_{SZ}v))\|_{L_2(K)}^2$$

for each element $K \in \mathcal{T}_h$. Since $\mathfrak{I}_{SZ}v$ is a linear polynomial and ν is piecewise constant, we deduce

$$\operatorname{div}_x(\nu \nabla_x(\mathfrak{I}_{SZ}v)) = \nu_K \operatorname{div}_x(\nabla_x(\mathfrak{I}_{SZ}v)) = 0$$

for each element $K \in \mathcal{T}_h$. Hence, we get

$$\sum_{K \in \mathcal{T}_h} \theta_K h_K \|\operatorname{div}_x(\nu \nabla_x v)\|_{L_2}^2 = \sum_{K \in \mathcal{T}_h} h_K^{2(l-1)} \theta_K h_K^{1-2(l-1)} \|\operatorname{div}_x(\nu \nabla_x v)\|_{L_2(K)}^2,$$

where the norm is bounded since $v \in V_0$. Moreover, for $\theta_K = \mathcal{O}(h_K)$, the term $\theta_K h_K^{1-2(l-1)}$ is bounded for $1 \leq l \leq 2$, and the case $l > 2$ is already treated in [8]. Combining all above estimates, we obtain

$$\begin{aligned} \|v - \mathfrak{I}_{SZ}v\|_{h,*}^2 &\leq c_2 \sum_{K \in \mathcal{T}_h} h_K^{2(l-1)} |v|_{H^l(S_K)}^2 + \sum_{K \in \mathcal{T}_h} C_{\mathfrak{I}_{SZ}}^2 \left(\frac{h_K}{\theta_K}\right) h_K^{2(l-1)} |v|_{H^l(S_K)}^2 \\ &\quad + \sum_{K \in \mathcal{T}_h} (\theta_K h_K^{3-2l}) h_K^{2(l-1)} \|\operatorname{div}_x(\nu \nabla_x v)\|_{L_2(K)}^2 \\ &\leq c_3 \sum_{K \in \mathcal{T}_h} h_K^{2(l-1)} \left(|v|_{H^l(S_K)}^2 + \|\operatorname{div}_x(\nu \nabla_x v)\|_{L_2(K)}^2 \right), \end{aligned}$$

with $c_3 = c_2 + \max_{K \in \mathcal{T}_h} \{C_{\mathfrak{I}_{SZ}}^2 (h_K/\theta_K), \theta_K h_K^{3-2l}\}$. For the general case of higher order basis functions, i.e., $p \geq 2$, the divergence of the gradient does not vanish. First we split the divergence of the gradient and also the norms, obtaining

$$\begin{aligned} &\sum_{K \in \mathcal{T}_h} \theta_K h_K \|\operatorname{div}_x(\nu \nabla_x v) - \operatorname{div}_x(\nu \nabla_x(\mathfrak{I}_{SZ}v))\|_{L_2}^2 \\ &\leq \sum_{K \in \mathcal{T}_h} 2\theta_K h_K \left(\|\operatorname{div}_x(\nu \nabla_x v)\|_{L_2}^2 + \|\operatorname{div}_x(\nu \nabla_x(\mathfrak{I}_{SZ}v))\|_{L_2}^2 \right) \end{aligned}$$

The first term in the sum we have already estimated above, where we now replace l by $s = \min\{l, p+1\}$, which is in our case ($l \leq 2$) again just l . For the second term, we insert $\nu_K \operatorname{div}_x(\nabla_x(\mathfrak{I}_{SZ}^1 v))$ into the norm, where $\mathfrak{I}_{SZ}^1 v$ is the linear quasi-interpolation of v . We observe that $\mathfrak{I}_{SZ}^1 v - \mathfrak{I}_{SZ}v$ is a finite element function, i.e., we can apply the inverse equality for the $H(\operatorname{div}_x)$ -norm [8, Lemma 3.5]. Since the diffusion coefficient is piecewise constant, we obtain

$$\begin{aligned} &\sum_{K \in \mathcal{T}_h} 2\theta_K h_K \|\operatorname{div}_x(\nu \nabla_x(\mathfrak{I}_{SZ}^1 v - \mathfrak{I}_{SZ}v))\|_{L_2}^2 \\ &\leq \sum_{K \in \mathcal{T}_h} 2\theta_K h_K h_K^{-2} c_{I,3}^2 \|\nu \nabla_x(\mathfrak{I}_{SZ}^1 v - \mathfrak{I}_{SZ}v)\|_{L_2(K)}^2 \\ &\leq \sum_{K \in \mathcal{T}_h} 2\theta_K h_K^{-1} c_{I,3}^2 \nu_K^2 \|\nabla_x(\mathfrak{I}_{SZ}^1 v - \mathfrak{I}_{SZ}v)\|_{L_2(K)}^2 \end{aligned}$$

Now we insert and subtract $\nabla_x v$ and use the triangle inequality, which yields

$$\begin{aligned} &\sum_{K \in \mathcal{T}_h} 2\theta_K h_K^{-1} c_{I,3}^2 \bar{\nu}_K^2 \|\nabla_x(\mathfrak{I}_{SZ}^1 v - \mathfrak{I}_{SZ}v)\|_{L_2(K)}^2 \\ &\leq \sum_{K \in \mathcal{T}_h} 4\theta_K h_K^{-1} c_{I,3}^2 \bar{\nu}_K^2 \left(\|\nabla_x(v - \mathfrak{I}_{SZ}^1 v)\|_{L_2(K)}^2 + \|\nabla_x(v - \mathfrak{I}_{SZ}v)\|_{L_2(K)}^2 \right). \end{aligned}$$

For both terms we can apply (10) (quasi-interpolation) and obtain

$$\begin{aligned}
& \sum_{K \in \mathcal{T}_h} 4\theta_K h_K^{-1} c_{I,3}^2 \nu_K^2 \left(\|\nabla_x(v - \mathfrak{I}_{SZ}^1 v)\|_{L_2(K)}^2 + \|\nabla_x(v - \mathfrak{I}_{SZ} v)\|_{L_2(K)}^2 \right) \\
& \leq \sum_{K \in \mathcal{T}_h} 4\theta_K h_K^{-1} c_{I,3}^2 \nu_K^2 \left(C_{\mathfrak{I}_{SZ}}^2 h_K^{2(l-1)} |v|_{H^l(S_K)}^2 + C_{\mathfrak{I}_{SZ}}^2 h_K^{2(l-1)} |v|_{H^l(S_K)}^2 \right) \\
& \leq \sum_{K \in \mathcal{T}_h} 8\theta_K h_K^{-1} c_{I,3}^2 \nu_K^2 C_{\mathfrak{I}_{SZ}}^2 h_K^{2(l-1)} |v|_{H^l(S_K)}^2.
\end{aligned}$$

Combining all of the above,

$$\begin{aligned}
& \|v - \mathfrak{I}_{SZ} v\|_{h,*}^2 \\
& \leq c_2 \sum_{K \in \mathcal{T}_h} h_K^{2(l-1)} |v|_{H^l(S_K)}^2 + \sum_{K \in \mathcal{T}_h} 2(\theta_K h_K^{3-2l}) h_K^{2(l-1)} \|\operatorname{div}_x(\nu \nabla_x v)\|_{L_2(K)}^2 \\
& \quad + \sum_{K \in \mathcal{T}_h} (8\theta_K h_K^{-1} c_{I,3}^2 \nu_K^2 C_{\mathfrak{I}_{SZ}}^2) h_K^{2(l-1)} |v|_{H^l(S_K)}^2 \\
& \leq c_{3,p} \sum_{K \in \mathcal{T}_h} h_K^{2(l-1)} \left(|v|_{H^l(S_K)}^2 + \|\operatorname{div}_x(\nu \nabla_x v)\|_{L_2(K)}^2 \right),
\end{aligned}$$

where $c_{3,p} = c_2 + \max_{K \in \mathcal{T}_h} \{8\theta_K h_K^{-1} c_{I,3}^2 \nu_K^2 C_{\mathfrak{I}_{SZ}}^2, 2(\theta_K h_K^{3-2l})\}$. \square

Now we are in the position to prove our main theorem.

Theorem 3. *Let p be the polynomial degree used, and let $u \in H^l(Q) \cap V_0$, with $l > 1$, be the exact solution, and $u_h \in V_{0h}$ be the approximate solution of the finite element scheme (3). Furthermore, let the assumptions of Lemma 1 (Céa-like estimate) and 2 (quasi-interpolation estimates) hold. Then the a priori discretization error estimate*

$$\|u - u_h\|_h \leq C \left(\sum_{K \in \mathcal{T}_h} h_K^{2(s-1)} (|u|_{H^s(S_K)}^2 + \|\operatorname{div}_x(\nu \nabla_x u)\|_{L_2(K)}^2) \right)^{1/2}, \quad (14)$$

holds, with $s = \min\{l, p + 1\}$ and a positive generic constant C .

Proof. Choosing the quasi-interpolant $v_h = \mathfrak{I}_{SZ} u$ in (9), we can apply the quasi-interpolation estimate (13) to obtain

$$\begin{aligned}
\|u - u_h\|_h & \leq \left(1 + \frac{\mu_b}{\mu_c} \right) \|u - \mathfrak{I}_{SZ} u\|_{h,*} \\
& \leq c_3 \left(1 + \frac{\mu_b}{\mu_c} \right) \left(\sum_{K \in \mathcal{T}_h} h_K^{2(s-1)} (|u|_{H^s(S_K)}^2 + \|\operatorname{div}_x(\nu \nabla_x u)\|_{L_2(K)}^2) \right)^{1/2}.
\end{aligned}$$

We set $C = c_3(1 + \mu_b/\mu_c)$ to obtain (14), which closes the proof. \square

5 Numerical results

We implemented the space-time finite element scheme (3) in C++, where we used the finite element library MFEM¹ and the solver library *hypre*². The linear system was solved by means of the GMRES method, preconditioned by the algebraic multigrid *BoomerAMG*. We stopped the iterative procedure if the initial residual was reduced by a factor of 10^{-8} . Both libraries are already fully parallelized with the Message Passing Interface (MPI). Therefore, we performed all numerical tests on the distributed memory cluster RADON1³ in Linz. For each element $K \in \mathcal{T}_h$, we choose $\theta_K = h_K/(\tilde{c}^2 \bar{\nu}_K)$, where \tilde{c} is computed by solving a local generalized eigenvalue problem which comes from an inverse inequality, see [8] for further details.

5.1 Example: Highly oscillatory solution

As first test example, we consider the unit (hyper-)cube $Q = (0, 1)^{d+1}$, with $d = 2, 3$, as space-time cylinder, and $\nu \equiv 1$. The manufactured function

$$u(x, t) = \sin\left(\frac{1}{\frac{1}{10\pi} + \sqrt{\sum_{i=1}^d x_i^2 + t^2}}\right)$$

serves as the exact solution, where we compute the right hand side f accordingly. This solution is highly oscillatory. Hence, we do not expect optimal rates for uniform refinement in the pre-asymptotic range. However, using adaptive refinement, we may be able to recover the optimal rates. We used the residual based error indicator proposed by Steinbach and Yang in [10]. For each element $K \in \mathcal{T}_h$, we compute

$$\eta_K^2 := h_K^2 \|R_h(u_h)\|_{L_2(K)}^2 + h_K \|J_h(u_h)\|_{L_2(\partial K)}^2,$$

where u_h is the solution of (3), $R_h(u_h) := f + \operatorname{div}_x(\nu \nabla_x u_h) - \partial_t u_h$ in K , and $J_h(u_h) := [\nu \nabla_x u_h]_e$ on $e \subset \partial K$, with $[\cdot]_e$ denoting the jump across one face $e \subset \partial K$. We mark each element where the condition $\eta_K \geq \sigma \max_{K \in \mathcal{T}_h} \eta_K$ is fulfilled, with σ an a priori chosen threshold, e.g., $\sigma = 0.5$. Note that $\sigma = 0$ results in uniform refinement. In Figure 1, we observe indeed reduced convergence rates for all polynomial degrees and dimensions tested. However, using an adaptive procedure, we are able to recover the optimal rates. Moreover, we significantly reduce the number of dofs required to reach a certain error threshold. For instance, in the case $d = 3$ and $p = 2$, we need 276 922 881 dofs to get an error in the $\|\cdot\|_h$ -norm of $\sim 10^{-1}$, whereas we only need 26 359 dofs with adaptive refinement. In terms of runtime, the uniform refinement needed 478.57s for assembling and solving, while the complete adaptive procedure took 156.5s only. The parallel performance is also shown in Figure 1, where we obtain a nice strong

¹<http://mfem.org/>

²<https://www.llnl.gov/casc/hypre/>

³<https://www.ricam.oeaw.ac.at/hpc/>

scaling up to 64 cores. Then the local problems are too small (only ~ 10000 dofs for 128 cores) and the communication overhead becomes too large.

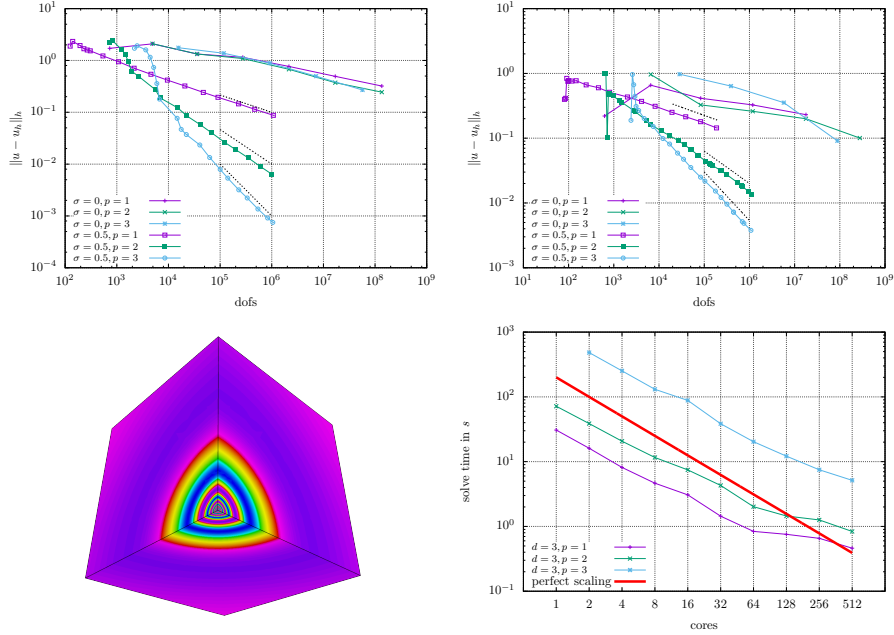


Figure 1: Example 5.1: Error rates in the $\|\cdot\|_h$ -norm for $d = 2$ (upper left) and $d = 3$ (upper right), the dotted lines indicate the optimal rate; Plot of the approximate solution u_h centered at the origin $(0,0,0)$ [8] (lower left); Strong scaling on a mesh with 1 185 921 dofs for $p = 1, 2$ and 5 764 801 dofs for $p = 3$ (lower right).

5.2 Example: Moving peak

For the second example, we consider the unit-cube $Q = (0, 1)^3$, i.e. $d = 2$. As diffusion coefficient, the choice $\nu \equiv 1$ is made. We choose the function

$$u(x, t) = (x_1^2 - x_1)(x_2^2 - x_2)e^{-100((x_1-t)^2+(x_2-t)^2)},$$

as exact solution and compute all data accordingly. This function is smooth, and almost zero everywhere, except in a small region around the line from the origin $(0,0,0)$ to $(1,1,1)$. This motivates again the use of an adaptive method. We use the residual based indicator η_K introduced in Example 5.1. In Figure 2, we can observe that we indeed obtain optimal rates for both uniform and adaptive refinement. However, using the a posteriori error indicator, we reduce the number of dofs needed to reach a certain threshold by one order of magnitude. For instance, in the case $p = 2$, we need 16 974 593 dofs to obtain

an error of $\sim 7 \times 10^{-5}$ with uniform refinement. Using adaptive refinement, we need 1 066 777 dofs only.

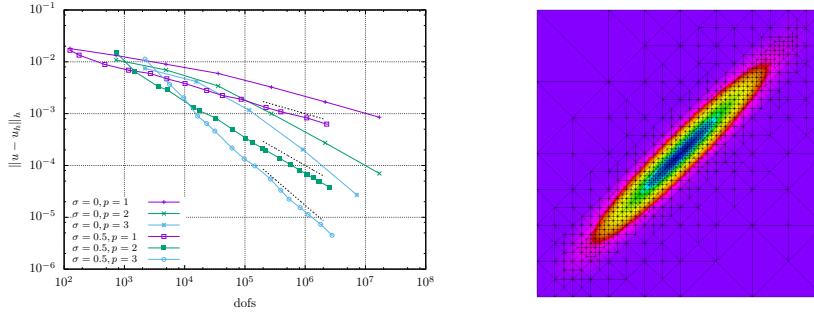


Figure 2: Example 5.2: Error rates in the $\|\cdot\|_h$ -norm for $d = 2$, the dotted lines indicate the optimal rates (left); Diagonal cut through the space-time mesh \mathcal{T}_h along the line from $(0, 0, 0)$ to $(1, 1, 1)$ after 8 adaptive refinements (right).

6 Conclusions

Following [8], we introduced a space-time finite element solver for non-autonomous parabolic evolution problems on completely unstructured simplicial meshes. We only assumed that we have so-called maximal parabolic regularity, i.e., the PDE is well posed in L_2 . We note that this property is only required locally in order to derive a consistent space-time finite element scheme. We extended the a priori error estimate in the mesh-dependent energy norm to the case of non-smooth solutions, i.e. $u \in H^{1+\epsilon}(Q)$, with $0 < \epsilon \leq 1$. This is necessary, since we cannot expect a smooth solution, especially when dealing with discontinuous diffusion coefficients. For simplicity, we considered only piecewise constant diffusion coefficients. The extension to piecewise smooth coefficients is straight-forward, but more technical. In comparison to the previous result for sufficiently smooth solutions, we no longer have a completely localized estimate. We also have to include the neighborhood of an element $K \in \mathcal{T}_h$. This may not be sufficient if we have to deal with solutions that have different regularity in different subdomains of the whole space-time cylinder. In applications, these subdomains correspond, for instance, to different materials. However, Duan et al. [5] have shown a quasi-interpolation estimate that fits into this setting.

We performed two numerical examples with known solutions. The first example had a highly oscillatory solution, and the second one was almost zero everywhere except along a line through the space-time cylinder. Using a high-performance cluster, we solved both problems on a sequence of uniformly refined meshes, where we also obtained good strong scaling rates. In order to reduce the computational cost, we also applied an adaptive procedure, using a residual based error indicator. Indeed, using a simultaneously in space and time adaptive procedure reduced the computational as well as the memory cost by a large factor.

Moreover, we could observe that, especially for $d = 3$, the AMG preconditioned GMRES method solves the problem quite efficiently.

References

- [1] R. E. BANK, P. VASSILEVSKI, AND L. ZIKATANOV, *Arbitrary dimension convection-diffusion scheme for space-time discretizations*, J. Comput. Appl. Math., 310 (2017), pp. 19–31.
- [2] S. C. BRENNER AND L. R. SCOTT, *The mathematical theory of finite element methods*, vol. 15 of Texts in Applied Mathematics, Springer, New York, third ed., 2008.
- [3] P. CLÉMENT, *Approximation by finite element functions using local regularization*, Rev. Française Automat. Informat. Recherche Opérationnelle Sér., 9 (1975), pp. 77–84.
- [4] D. DEVAUD AND C. SCHWAB, *Space-time hp-approximation of parabolic equations*, Calcolo, 55 (2018), p. 35.
- [5] H. DUAN, S. LI, R. C. E. TAN, AND W. ZHENG, *A delta-regularization finite element method for a double curl problem with divergence-free constraint*, SIAM J. Numer. Anal., 50 (2012), pp. 3208–3230.
- [6] S. FACKLER, *Non-autonomous maximal regularity for forms given by elliptic operators of bounded variation*, J. Differential Equations, 263 (2017), pp. 3533–3549.
- [7] O. A. LADYŽHENSKAYA, *The boundary value problems of mathematical physics*, vol. 49 of Applied Mathematical Sciences, Springer-Verlag, New York, 1985.
- [8] U. LANGER, M. NEUMÜLLER, AND A. SCHAFELNER, *Space-time Finite Element Methods for Parabolic Evolution Problems with Variable Coefficients*, in Advanced Finite Element Methods with Applications - Proceedings of the 30th Chemnitz FEM Symposium 2017, T. Apel, U. Langer, A. Meyer, and O. Steinbach, eds., LNCSE, Springer, Berlin, Heidelberg, New York, 2019. to appear.
- [9] O. STEINBACH, *Space-time finite element methods for parabolic problems*, Comput. Methods Appl. Math., 15 (2015), pp. 551–566.
- [10] O. STEINBACH AND H. YANG, *Space-time finite element methods for parabolic evolution equations: Discretization, a posteriori error estimation, adaptivity and solution*, in Space-Time Methods: Application to Partial Differential Equations, Radon Series on Computational and Applied Mathematics, de Gruyter, 2019. to appear.

Technical Reports of the Doctoral Program

“Computational Mathematics”

2019

- 2019-01** A. Seiler, B. Jüttler: *Approximately C^1 -smooth Isogeometric Functions on Two-Patch Domains* Jan 2019. Eds.: J. Schicho, U. Langer
- 2019-02** A. Jiménez-Pastor, V. Pillwein, M.F. Singer: *Some structural results on D^n -finite functions* Feb 2019. Eds.: M. Kauers, P. Paule
- 2019-03** U. Langer, A. Schafelner: *Space-Time Finite Element Methods for Parabolic Evolution Problems with Non-smooth Solutions* March 2019. Eds.: B. Jüttler, V. Pillwein

2018

- 2018-01** D. Dominici: *Laguerre-Freud equations for Generalized Hahn polynomials of type I* Jan 2018. Eds.: P. Paule, M. Kauers
- 2018-02** C. Hofer, U. Langer, M. Neumüller: *Robust Preconditioning for Space-Time Isogeometric Analysis of Parabolic Evolution Problems* Feb 2018. Eds.: U. Langer, B. Jüttler
- 2018-03** A. Jiménez-Pastor, V. Pillwein: *Algorithmic Arithmetics with DD-Finite Functions* Feb 2018. Eds.: P. Paule, M. Kauers
- 2018-04** S. Hubmer, R. Ramlau: *Nesterov’s Accelerated Gradient Method for Nonlinear Ill-Posed Problems with a Locally Convex Residual Functional* March 2018. Eds.: U. Langer, R. Ramlau
- 2018-05** S. Hubmer, E. Sherina, A. Neubauer, O. Scherzer: *Lamé Parameter Estimation from Static Displacement Field Measurements in the Framework of Nonlinear Inverse Problems* March 2018. Eds.: U. Langer, R. Ramlau
- 2018-06** D. Dominici: *A note on a formula of Krattenthaler* March 2018. Eds.: P. Paule, V. Pillwein
- 2018-07** C. Hofer, S. Takacs: *A parallel multigrid solver for multi-patch Isogeometric Analysis* April 2018. Eds.: U. Langer, B. Jüttler
- 2018-08** D. Dominici: *Power series expansion of a Hankel determinant* June 2018. Eds.: P. Paule, M. Kauers
- 2018-09** P. Paule, S. Radu: *A Unified Algorithmic Framework for Ramanujan’s Congruences Modulo Powers of 5, 7, and 11* Oct 2018. Eds.: M. Kauers, V. Pillwein
- 2018-10** D. Dominici: *Matrix factorizations and orthogonal polynomials* Nov 2018. Eds.: P. Paule, M. Kauers
- 2018-11** D. Dominici, V. Pillwein: *Difference equation satisfied by the Stieltjes transform of a sequence* Dec 2018. Eds.: P. Paule, M. Kauers
- 2018-12** N.A. Smoot: *A Family of Congruences for Rogers–Ramanujan Subpartitions* Dec 2019. Eds.: P. Paule, V. Pillwein

Doctoral Program

“Computational Mathematics”

Director:

Dr. Veronika Pillwein
Research Institute for Symbolic Computation

Deputy Director:

Prof. Dr. Bert Jüttler
Institute of Applied Geometry

Address:

Johannes Kepler University Linz
Doctoral Program “Computational Mathematics”
Altenbergerstr. 69
A-4040 Linz
Austria
Tel.: ++43 732-2468-6840

E-Mail:

office@dk-compmath.jku.at

Homepage:

<http://www.dk-compmath.jku.at>